Unraveling the packing pattern leading to gelation using SS NMR and X-ray diffraction: Direct observation of the evolution of self-assembled fibers

Nonappa,[a] Manu Lahtinen,*[a] Babita Behera,[a] Erkki Kolehmainen*[a] and Uday Maitra[b]

[a] Department of Chemistry, FI-40014, University of Jyväskylä, Finland.

[b]Department of Organic Chemistry, Indian Institute of Science, Bangalore-560 012.

Email: erkki.t.kolehmainen@jyu.fi, manu.k.lahtinen@jyu.fi

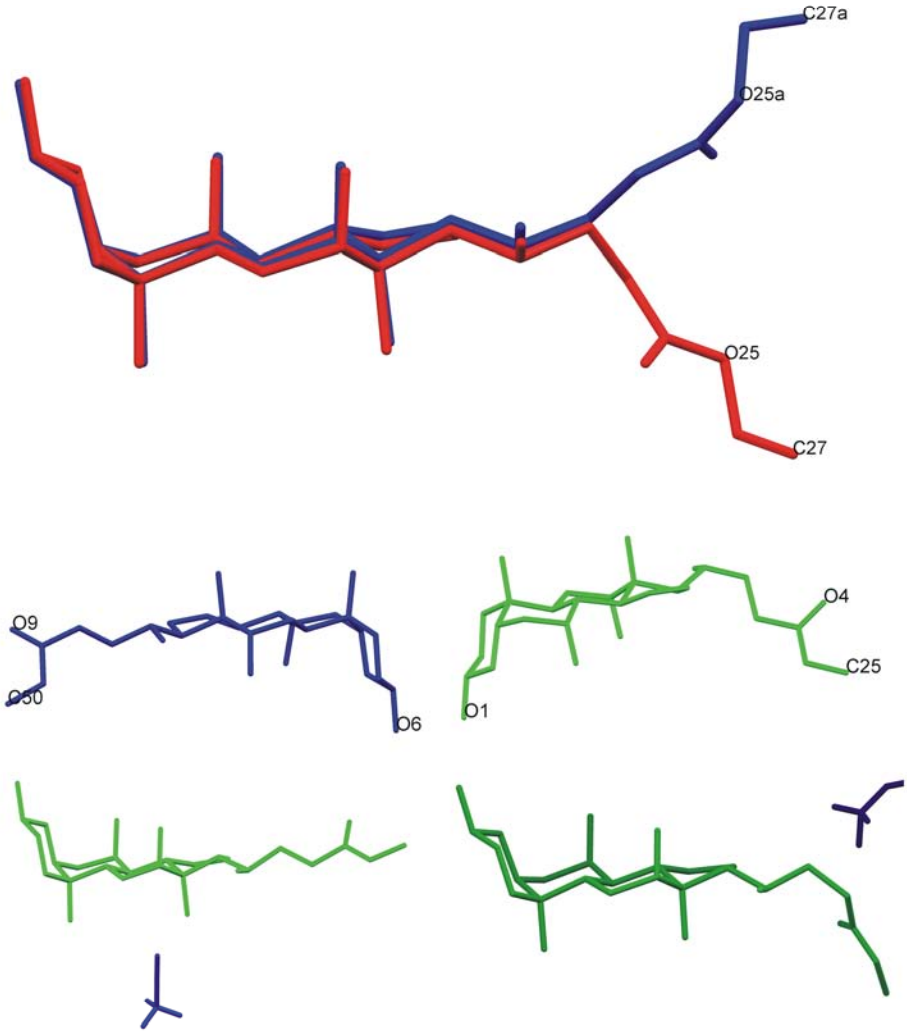

Figure S1. Top: conformational overlay of the two crystallographically independent molecules of compound **2**. Middle: conformations of solvate free methylcholate (YUTCEV) with two crystallographically independent molecules. Bottom left: methylcholate acetonitrile solvate (YUTCAR). Bottom right: methylcholate methanol solvate (FIVMIG10).

Comment. It can be noticed that the two different conformations of the side chain on compound **2** can be found also on methylcholates, as "boat"-conformation (colored red) can be seen on anhydrous methylcholate structure (YUTCEV), whereas the "chair" –conformation (colored blue) can be seen on methylcholate solvate (FIVMIG10). This for its part strengthens the correctness of the suggested powder structure of compound **2**, because similar kind molecular conformations seem to exist on other cholates esters as well. Similarly the second crystallographically independent conformation on the anhydrous methylcholate can be found on the methyl cholate acetonitrile solvate (YUTCAR), in which the side chain is leveled with the steroidal part.

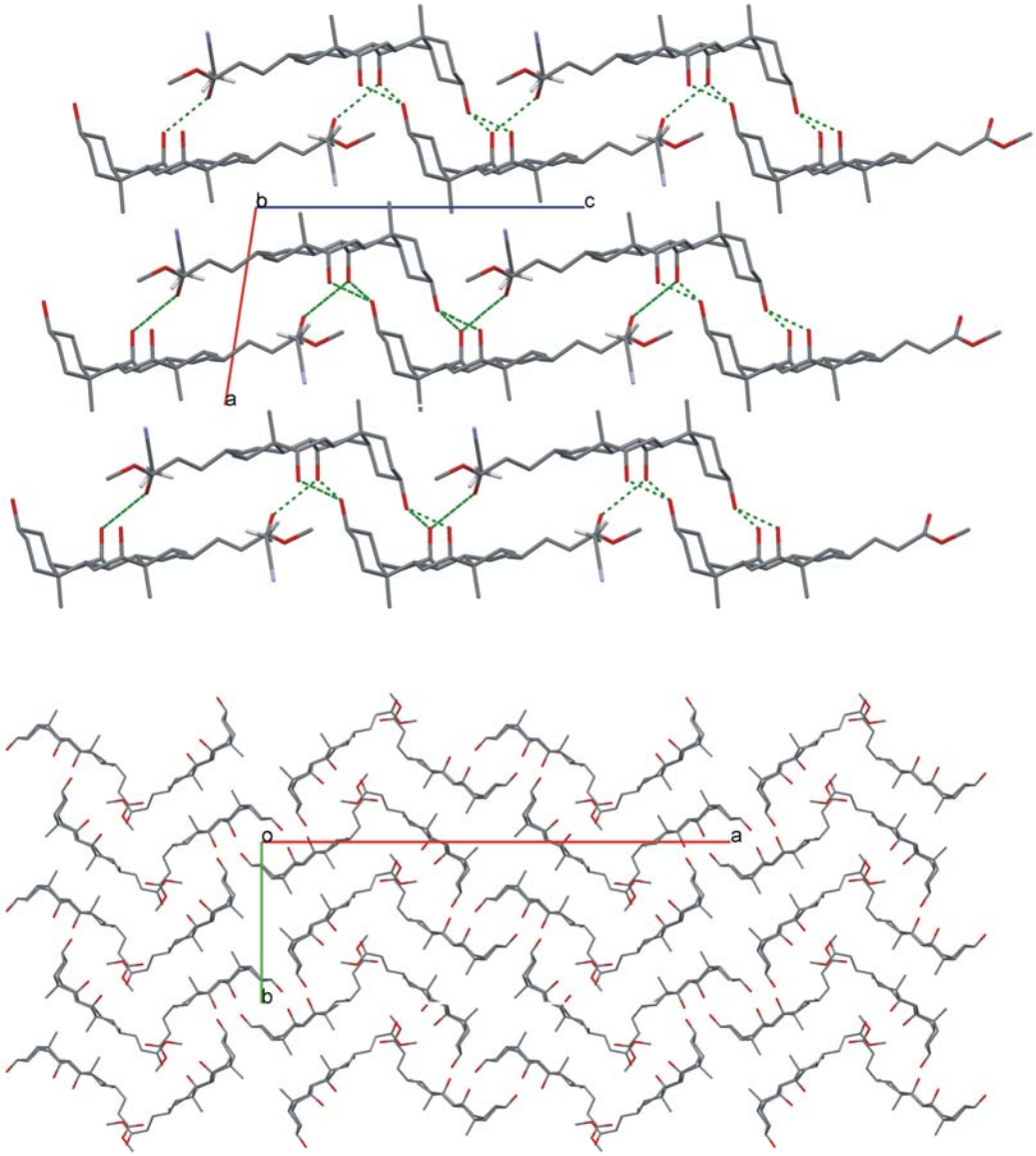

Figure S2. Top: Molecular packing of methylcholate acetonitrile solvate (YUTCAR) along *b*-axis. Bottom: Molecular packing of methylcholate (YUTCEV) along *c*-axis. The hydrogen bonding is shown by green dashed lines.

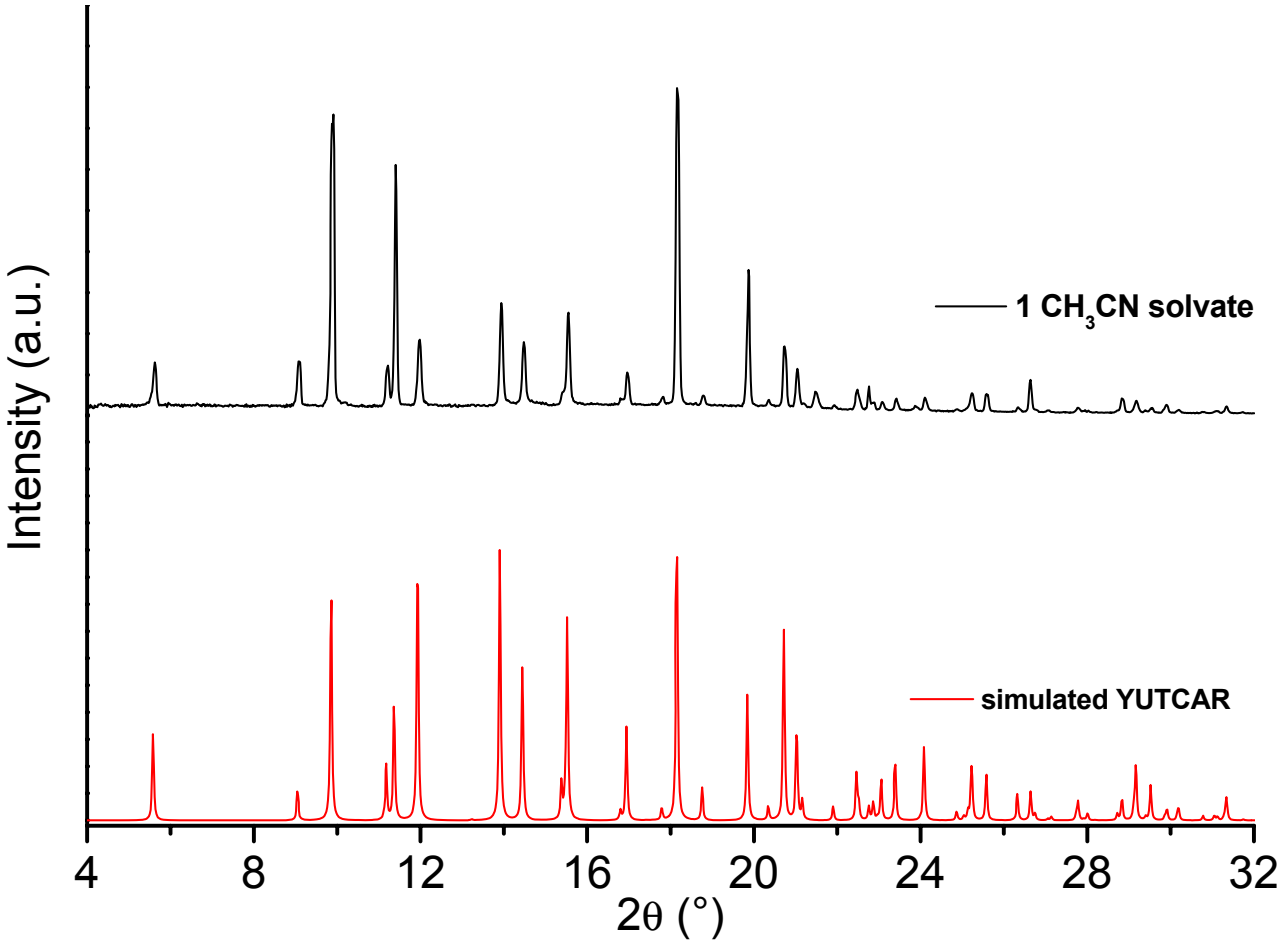

Figure S3. Experimental and simulated PXRD pattern of methyl cholate **1** acetonitrile solvate.

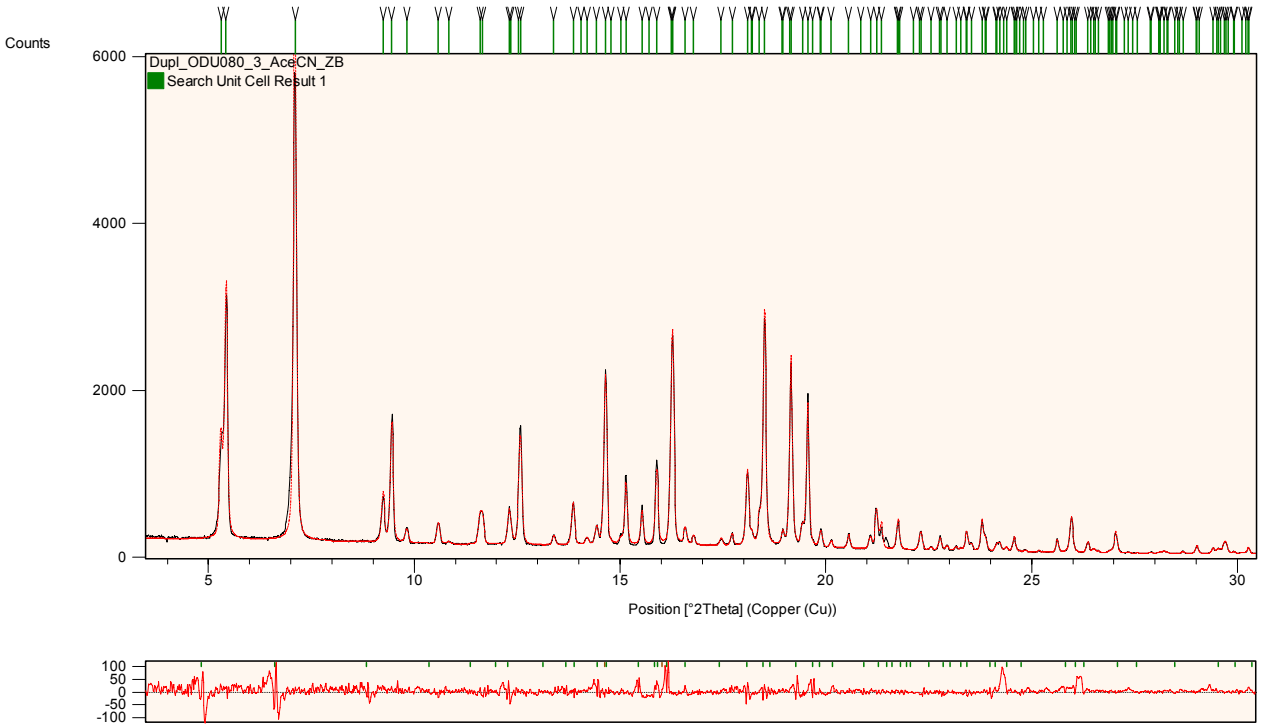

Figure S4. Le Bail fit of indexed ethyl cholate **2**.

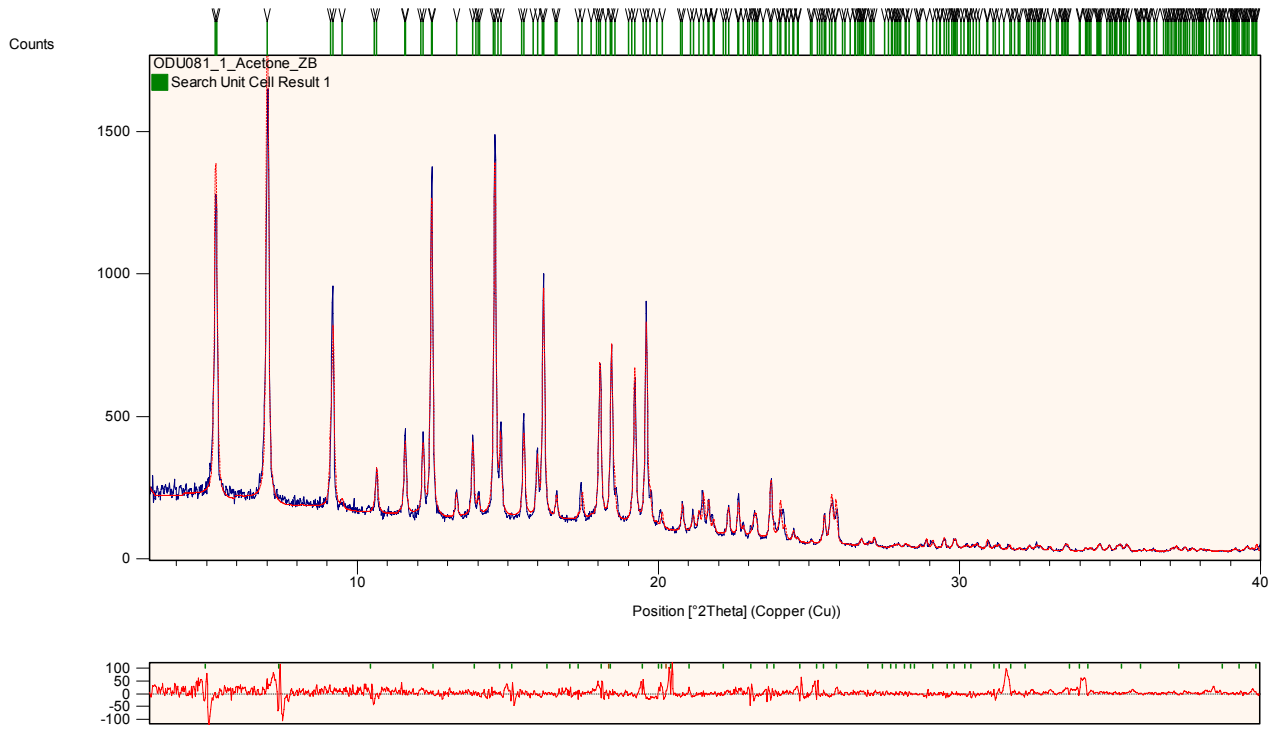

Figure S5. Le Bail fit of indexed propyl cholate **3**.

Experimental for powder structure determination

The instrumental resolution of the equipment was determined using highly crystalline silicon standard (SRM 640b, National Institute of Standards & Technology). For silicon, the sharpest half-width value of 0.04° (2θ) was obtained from diffraction peak on the 28.44° (2θ). The equipment was calibrated using mixture of LaB_6 (SRM 660, National Institute of Standards & Technology) and silicon standards so that an absolute error of less than 0.01° (2θ) on peak positions was achieved.

The structure determination of cholate **2** including data processing, peak search, indexing (DICVOL implemented in DASH), space group analysis and solving of the structure was made by the DASH v3.1 [5]. Diffraction data range of 3 – 30°C was used for indexing and range of 3.0-60° (2θ) structure determination. DASH program is based on simulated annealing method in which known structure moiety/moieties are needed to solve the structure. For ethyl and propyl cholates (**2**, **3**) entire cholate molecule including hydrogen atoms was used as the moiety and was generated by

molecular editor program Avogadro (v 0.9.7.),[1] using methyl cholate conformation from a known structure (YETCEW) as a starting point. Optimized geometry of the built molecule was produced by molecular mechanics in Avogadro. Z-matrices of two identical cholates were used on solving the structure, because the suggested unit cell volume (4919 or 5036 $Å^3$) together with most agreeable chiral space group no. 19 (4-fold symmetry) insist presence of two crystallographically different molecules in order to fill the entire unit cell volume. Typical estimate for number of formula units per unit cell (Z) is calculated by dividing cell volume (V) with number of non-hydrogen atoms multiplied by the average volume (18-20 $Å^3$) occupied by an atom in solid. In this case eight times 31 times 20 $Å^3$ = 4960 $Å^3$ and to achieve Z = 8 with 4-fold symmetry, atom coordinates of two molecules are needed (2 x 4 = 8). Due to large structure model (150 atoms altogether distributed in two separate molecules with 6 torsion angles, three position and four orientational variables on each molecule), the large search space was attempted to simplify by using the knowledge of chemically realistic bounds for particular torsion angles. The CSD was searched by MOGUL for chemically related compounds to find statistically the most common torsion angle ranges for the types of angles present in the ethyl cholate. For example, the torsion angle C24-C23-C22-C17 was restricted to vary within +- 20° around its initial angle, as in almost all structures found in the database the torsion angle C16-C17-C20-C21 is close to 180° (that torsion angle cannot be varied in the DASH program, directly). Similarly the torsion angle associated O=C-O-C ester group was restricted to vary with +- 10°. The final structure with most promising reduced chi2 value of 101 was revealed after 20 million simulated annealing moves.

Table S1. Crystallographic data of cholates **2** and **3**

Comp. Param.	**2**	**3**
a (Å)	7.8062(3)	7.8547(5)
b (Å)	18.7495(6)	19.470(1)
c (Å)	33.4892(6)	33.333(2)
α (°)	90	90
β (°)	90	90
γ (°)	90	90
V (Å^{-3})	4901.6	5097.7
SG (No.)	$2_12_12_1$ (19)	$2_12_12_1$ (19)
Temp (°C)	25	25
R_B (%) [a]	1.33	1.76
R_p (%) [b]	6.27	7.21
R_{wp} (%) [c]	8.38	9.65

a = Bragg factor, agreement between the reflection intensities calculated from a crystallographic model and those measured experimentally; b = profile factor, c = weighted profile factor. Values are obtained by Le Bail fit of the indexed data using HighScore Plus.

$$R_p = 100\left(\frac{\sum_{i=1,n}\left|y_i - y_{c,i}\right|}{\sum_{i=1,n} y_i}\right),\quad R_{wp} = 100\left(\frac{\sum_{i=1,n} w_i\left|y_i - y_{c,i}\right|^2}{\sum_{i=1,n} w_i y_i^{\,2}}\right)^{1/2},\quad R_B = 100\left(\sum_h \left|'I_{obs,h}' - I_{calc,h}\right| \Big/ \sum_h \left|'I_{obs,h}'\right|\right)$$

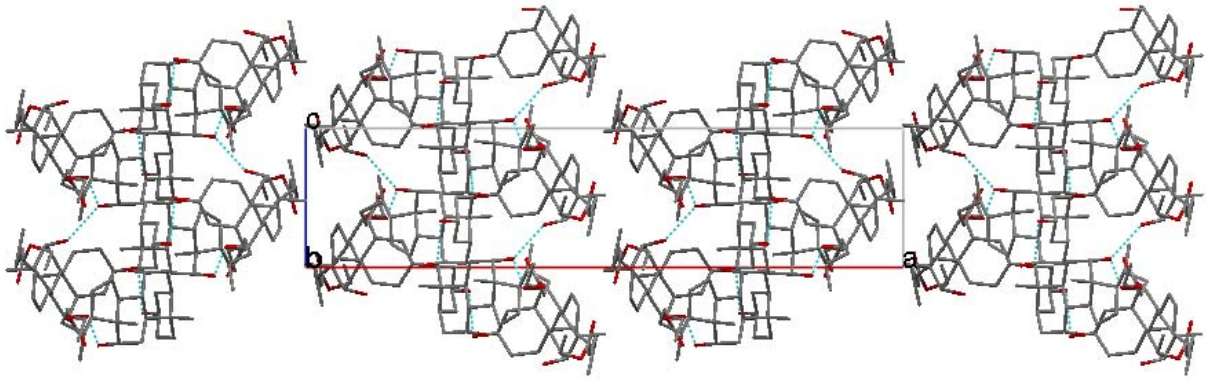

Figure S6. Molecular packing of ethyl cholate **2** along *b*-axis. Hydrogen bonding network between the cholates are highlighted by blue dashed lines. Hydrogen atoms are omitted for

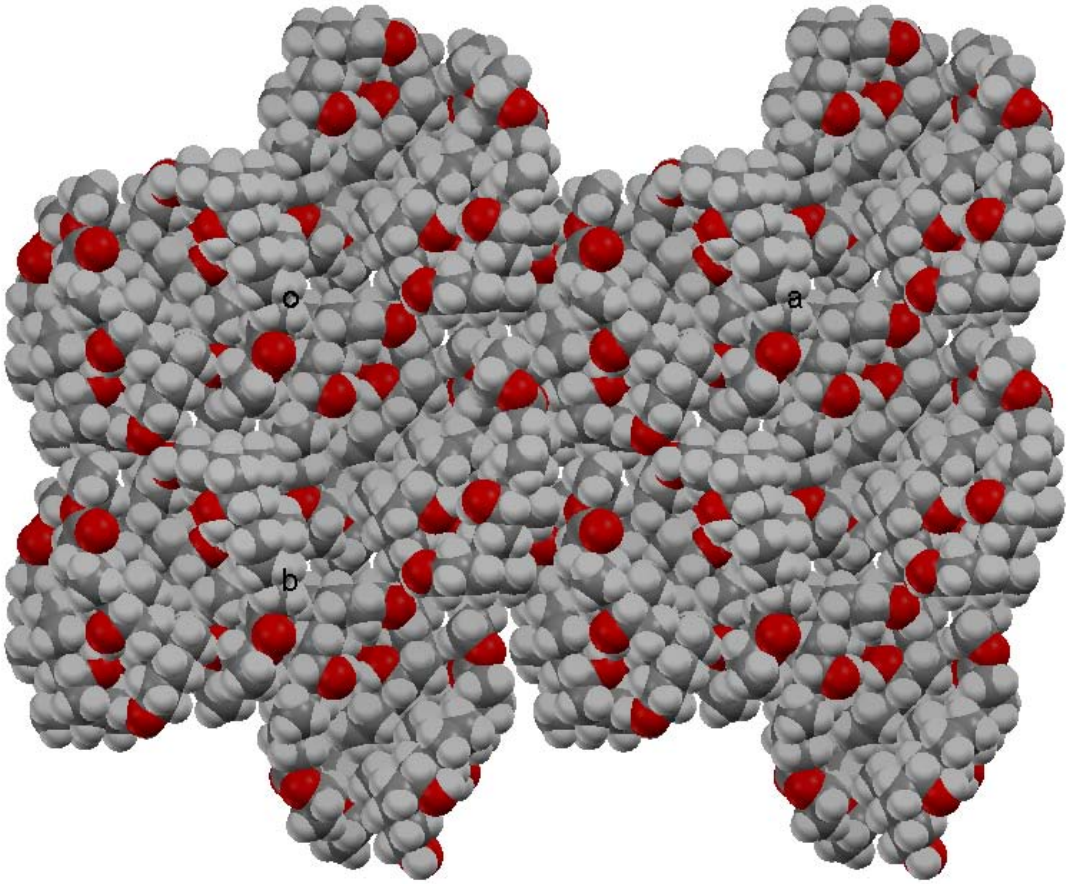

Figure S7. Spacefill presentation of ethyl cholate **2** along *c*-axis.

Table S2. Thermal properties of methyl cholate **1** acetonitrile solvate.

Specimen	Mw. g mol $^{-1}$	1st Heating T, (ΔH); T_g, [ΔC_p]	Melting points T_{m*} (T_{lit})$^{ref.}$	2nd heating T_x, (ΔH); T_g, [ΔC_p]	Decomp. T_d
1 – acetonitrile solvate	422.61 + 41.05	T_{dh} 87 – 99 (31.04), T_{ss} 110.2 (23.16), T_m 150.9 (59.72)	154.7 (154 – 156)[11]	T_g 71.2 [0.54],	262

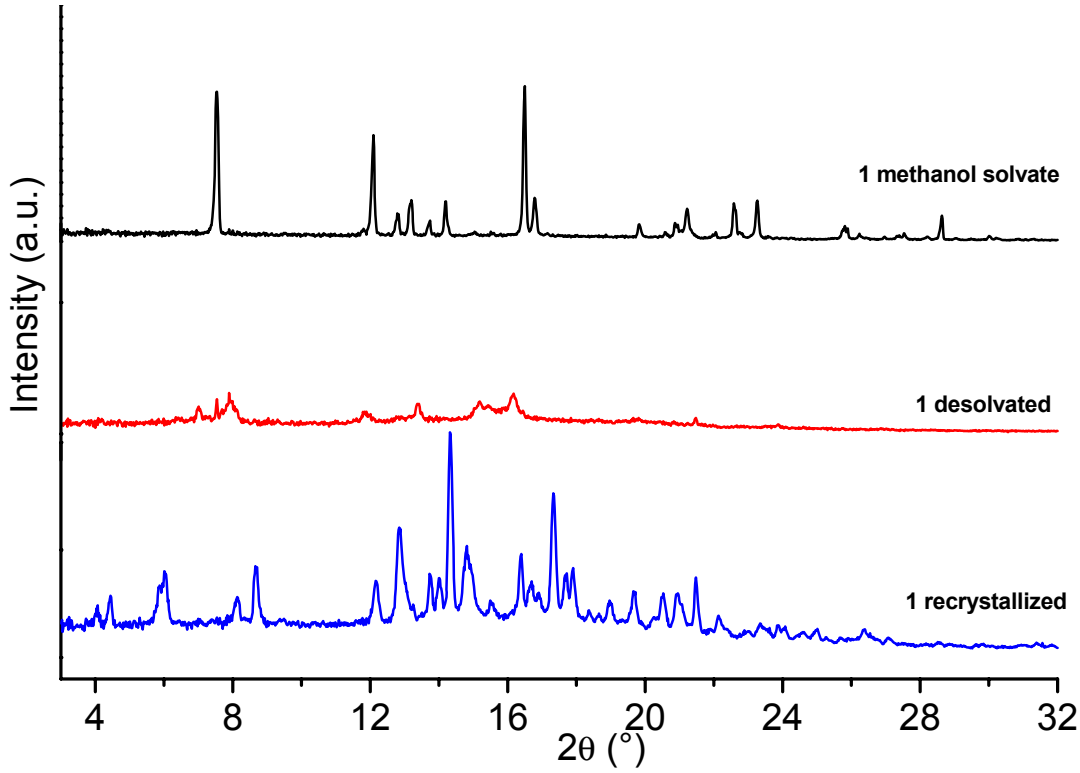

Figure S8. PXRD patterns of methyl cholate **1**, corresponding to a sample at room temperature, extracted at 90 °C and at 130°C, respectively.

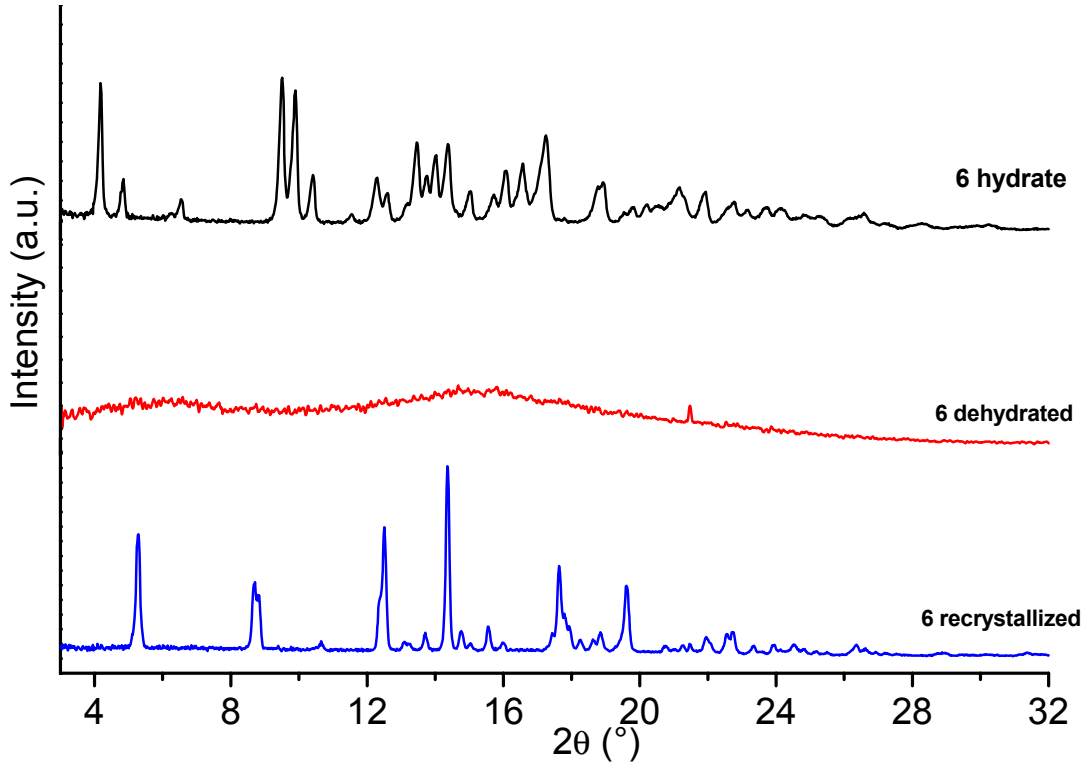

Figure S9. PXRD patterns of butyl cholate **6**, corresponding to a sample at room temperature, extracted at 70 °C and at 100°C, respectively.

Table S3. Thermal properties of compounds **1 – 6** obtained by DSC and TGA

Specimen	Mw. g mol $^{-1}$	1st Heating T, (ΔH); T_g, [ΔC_p]	Melting points T_{m*} (T_{lit})$^{ref.}$	2nd heating T_x, (ΔH); T_g, [ΔC_p]	Decomp. T_d
1 methanol solvate	422.61 + 32.04	T_{dh} 60 – 108 (99.06), T_{ss} 116.3 (5.54), T_m 147.8 (56.83)	152.6 (154 – 156)[11]	T_g 71.4 [0.44],	262
2	436.64	T_m 161.6 (92.83)	163.5 (162 – 164)[10]	T_g 64.4 [0.38], T_c 102.8 (-57.22), T_m 155.3 (76.53) *	253
3	450.66	T_m 158.7 (95.7)	161.7 (164 – 166)[10]	T_g 56.7 [0.36], T_c 96.5 (-59.72), T_m 159.4 (79.28)	253
4	448.65	T_m 156.2 (90.73)	157.7 (154 – 156)[10]	T_g 55.3 [0.42], T_c 87.4 (-52.98), T_m 156.2 (81.02)	267
5	446.63	T_m 140.5 (83.19)	144.0 (143 – 145)[10]	T_g 60.3 [0.37],	262
6	464.69 + xH_2O	T_{dh} 48 – 100 (125.10), [a] T_m 122.6 (33.66)	125.6 (125 – 126)[10]	T_g 50.4 [0.50]	267

T_{dh} = dehydration/ desolvation, T_{ss} = solid-solid phase transition, T_m = melting, T_c = cold crystallization (on heating) temperatures (°C) and its ΔH = enthalpy change (J g^{-1}); T_g = glass-transition (°C) and its ΔC_p = heat capacity change [J g^{-1} °C^{-1}]; T_{m*} = for comparison with a literature melting points are taken also as the peak maximum values; T_{lit} = literature values; T_d = decomposition onset temperature (°C); * = T_m of a polymorph. a = cold crystallization exotherm is overlapped by the evaporation endotherm (see text).

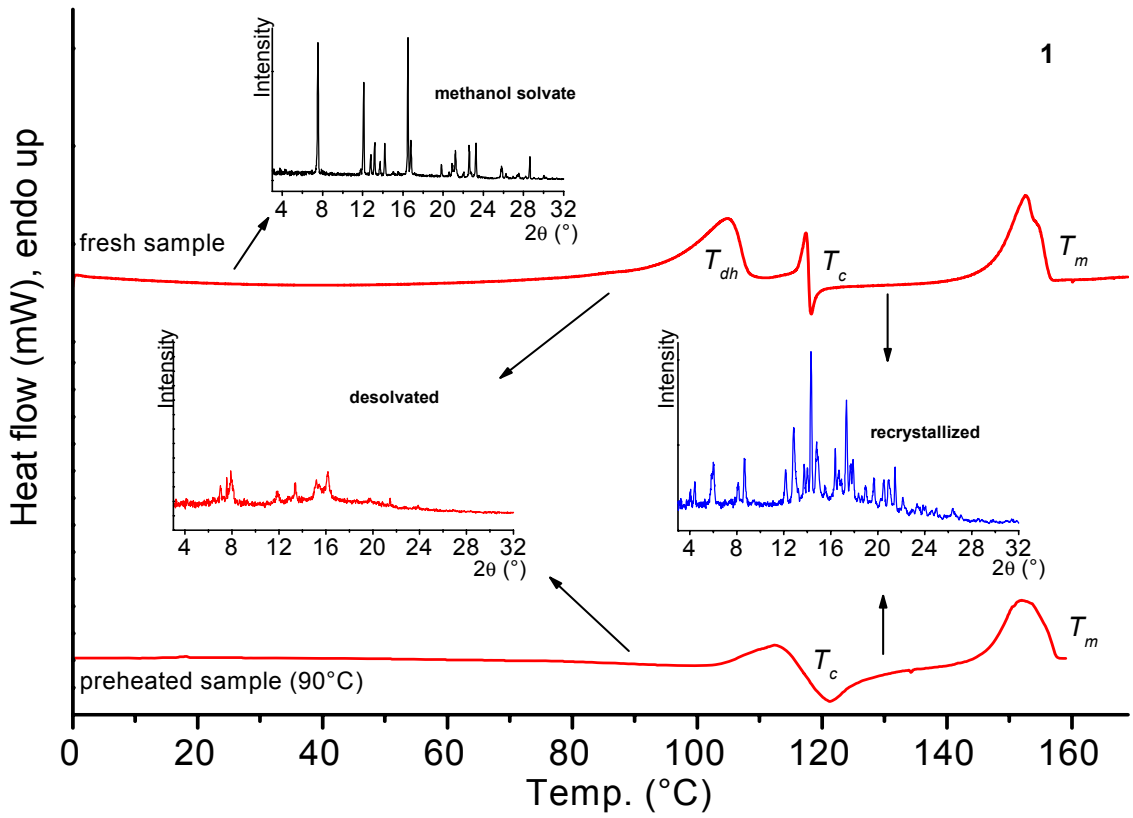

Figure S10. DSC scans of fresh and preheated (at 90 °C) samples of **1** together with embedded PXRD patterns of the samples extracted at room temperature, 90 °C and 130 °C

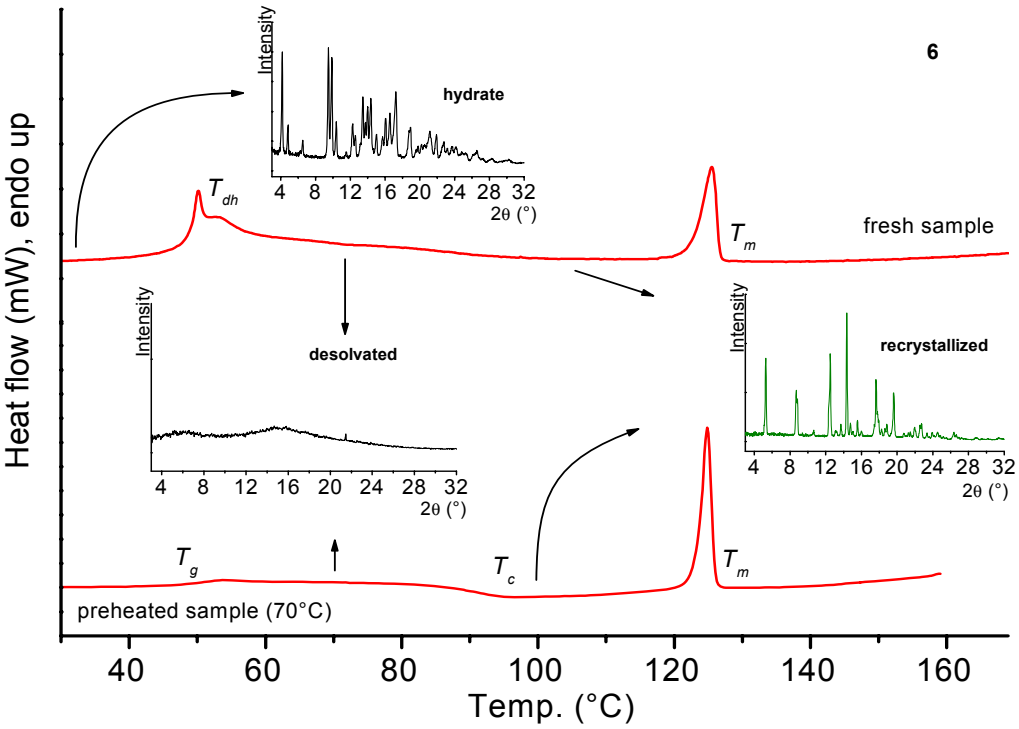

FigureS11. DSC scans of fresh and preheated (70 °C) samples of **6** together with embedded PXRD patterns of the samples extracted at room temperature, 70 °C and 100 °C.

^{13}C NMR in $CDCl_3$ at 125 MHz of **1** (MeOH solvate)

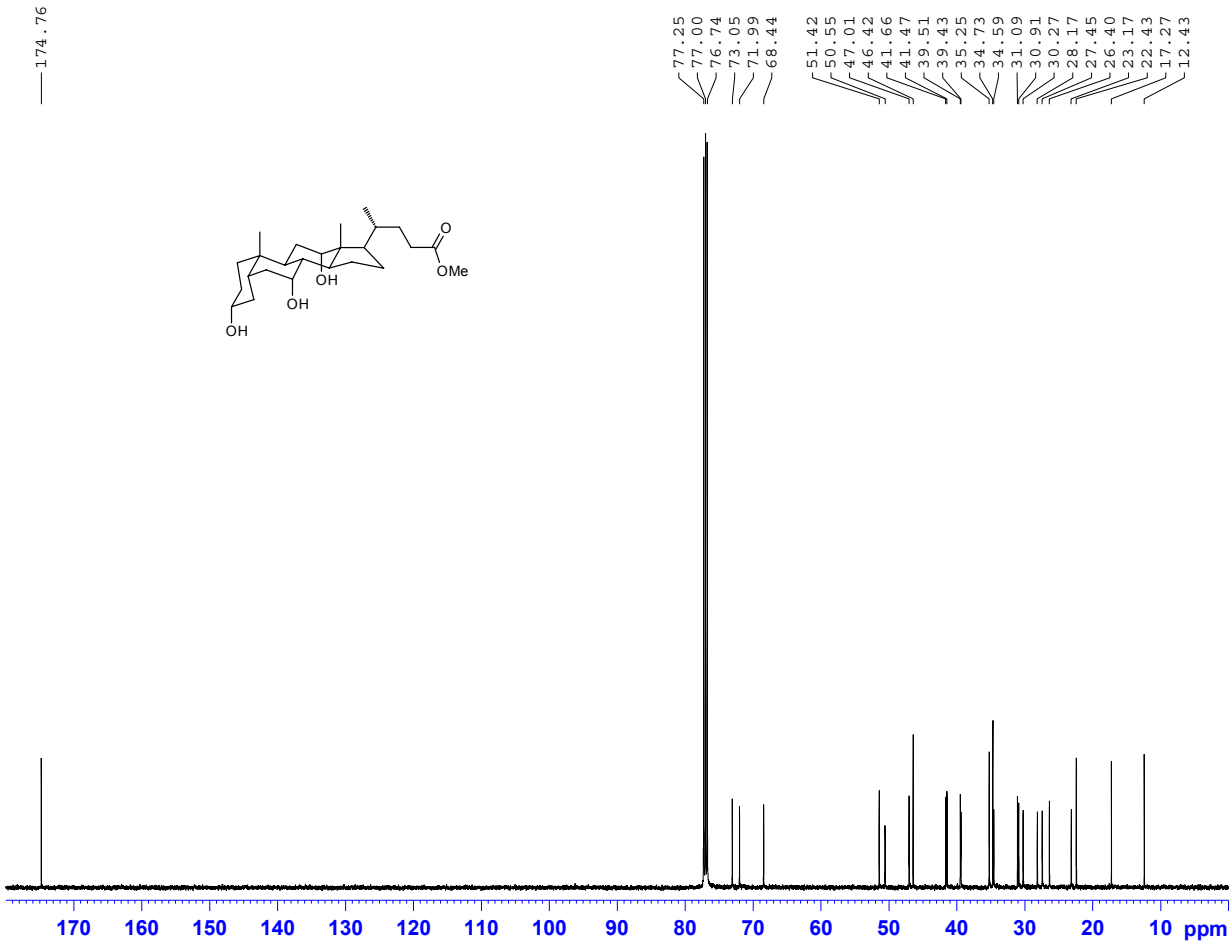

^{13}C NMR in $CDCl_3$ at 125 MHz of **1** (CH_3CN solvate)

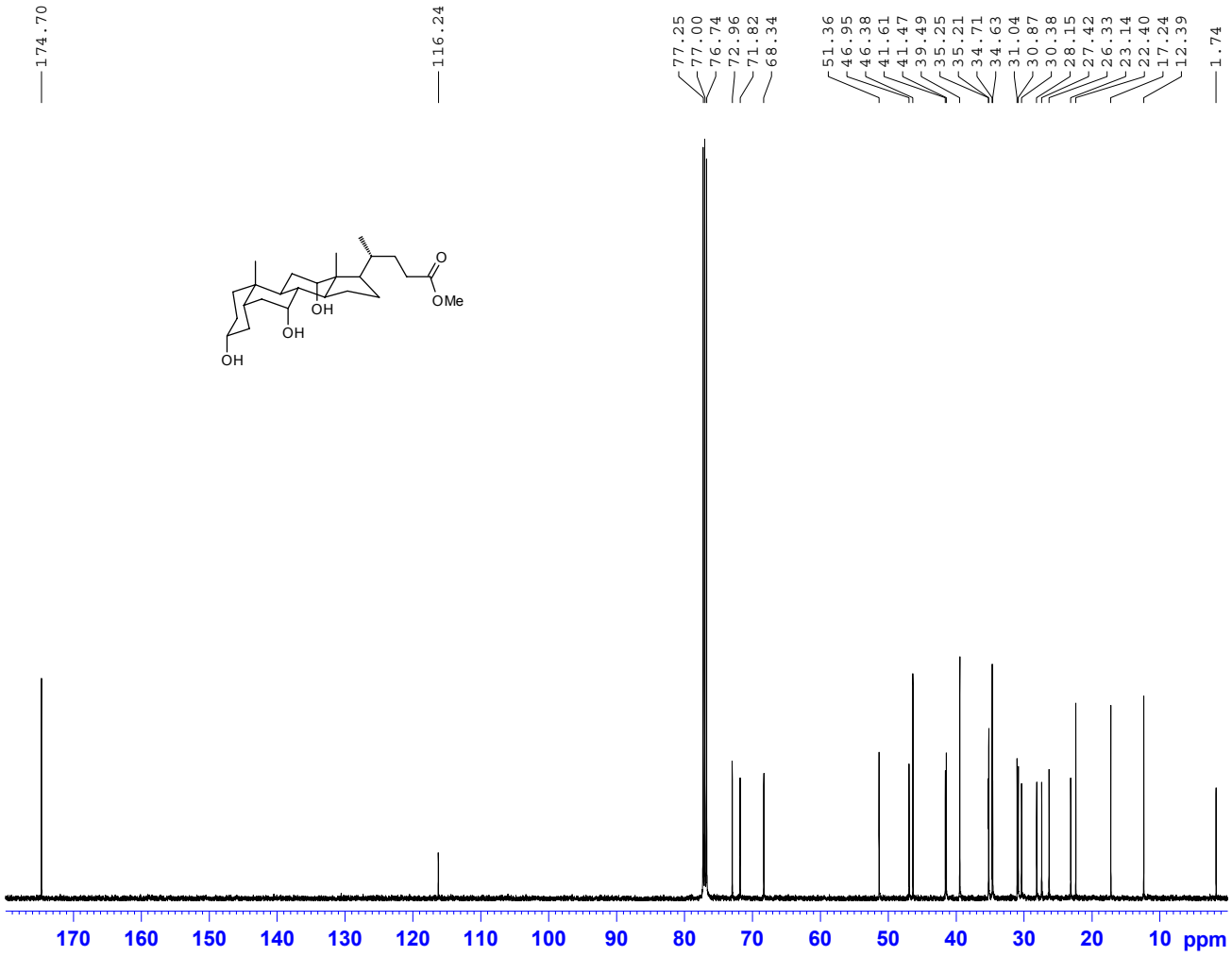

^{13}C NMR in $CDCl_3$ at 125 MHz of **2**

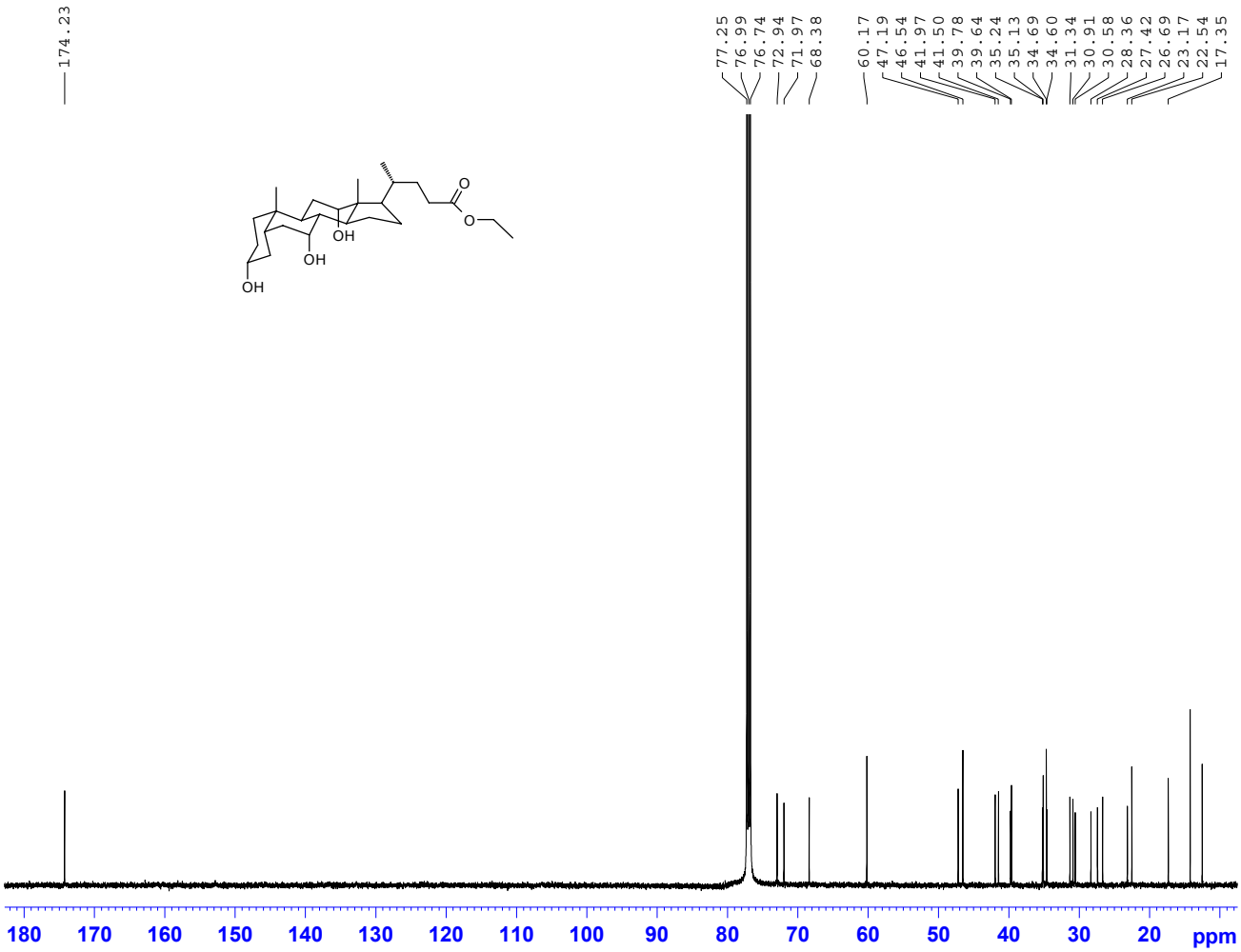

^{13}C NMR in $CDCl_3$ at 125 MHz of **3**

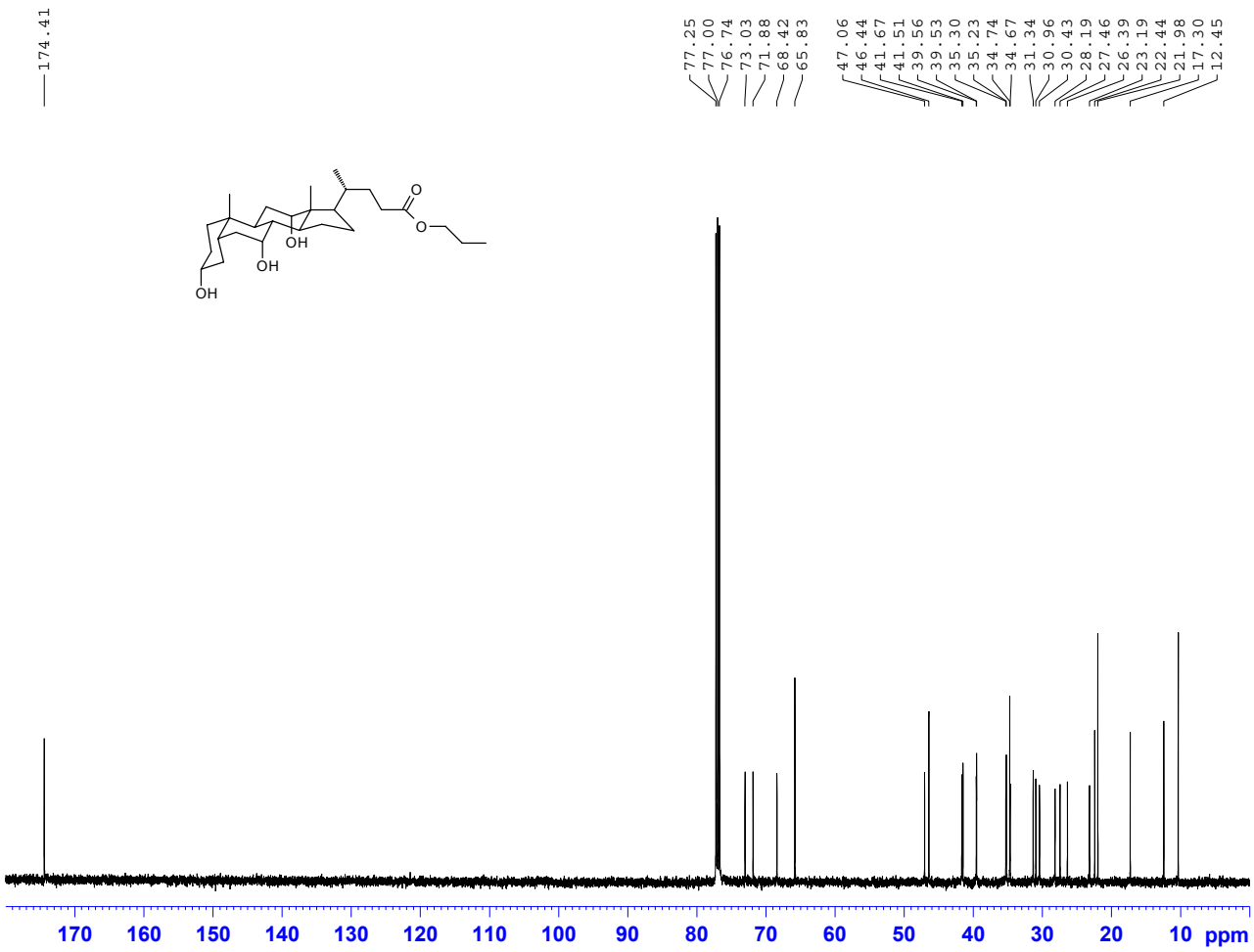

^{13}C NMR in $CDCl_3$ at 125 MHz of **4**

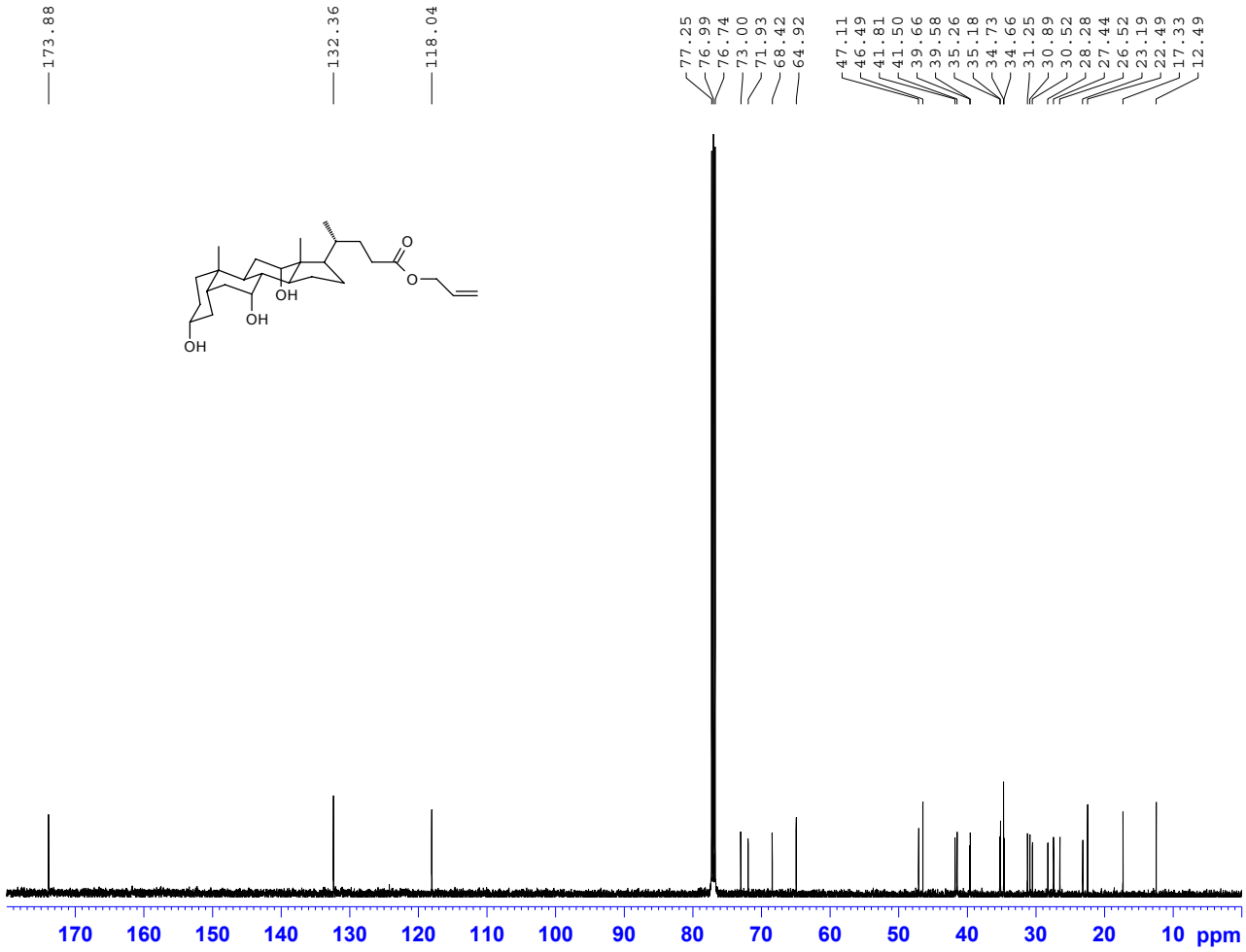

^{13}C NMR in $CDCl_3$ at 125 MHz of **5**

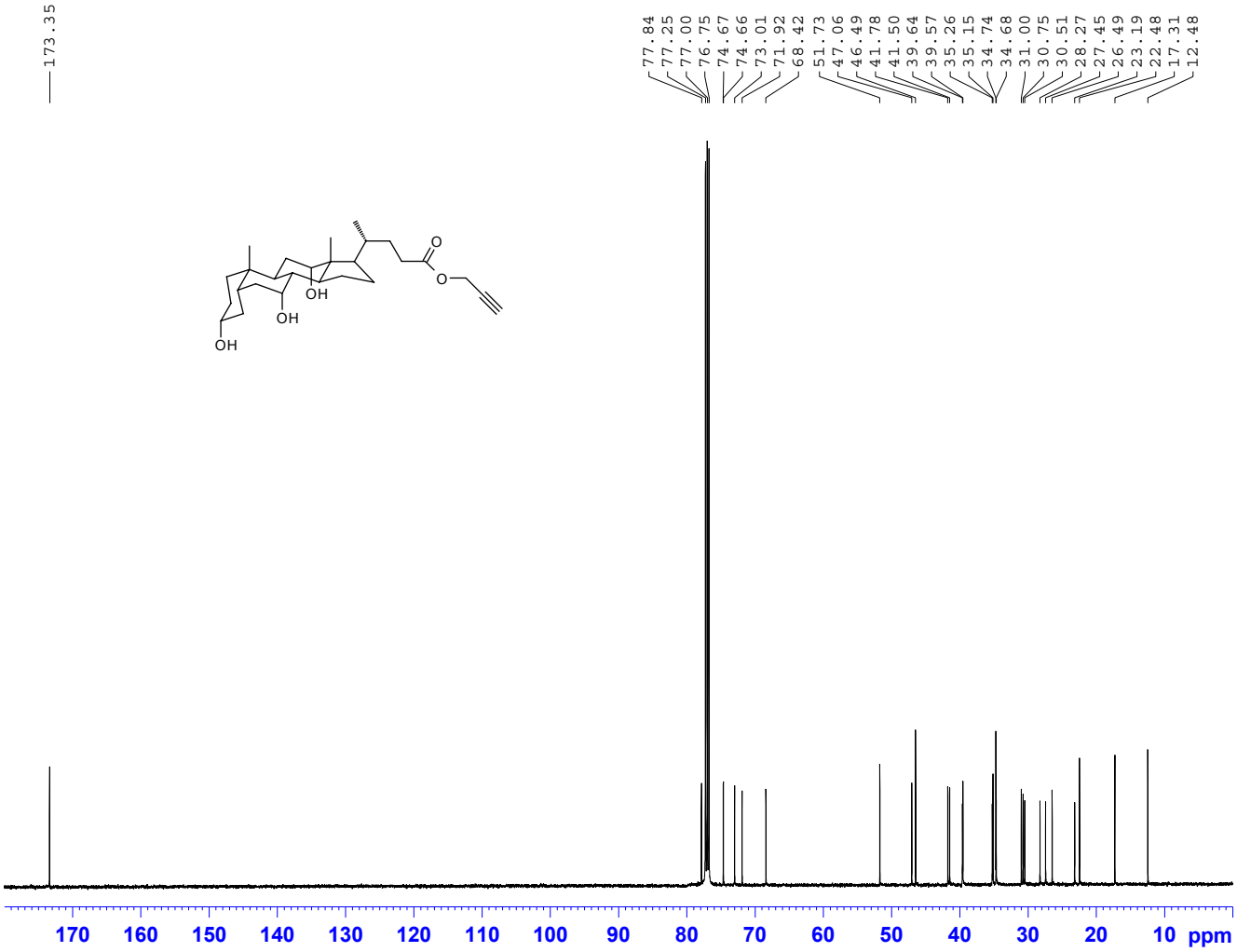

^{13}C NMR in $CDCl_3$ at 125 MHz of **6**

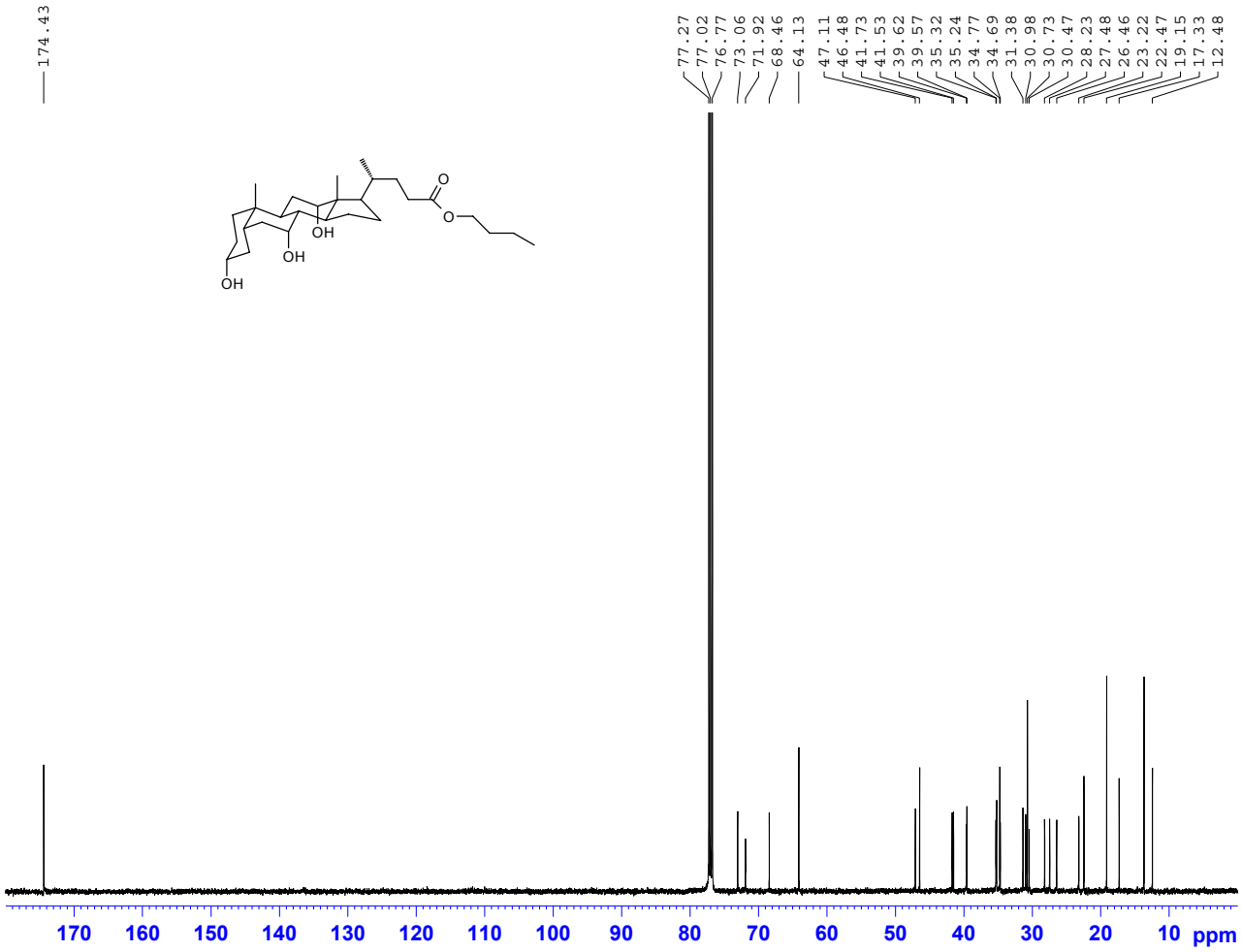

^{13}C CPMAS NMR spectra of **1** (MeOH Solvate)

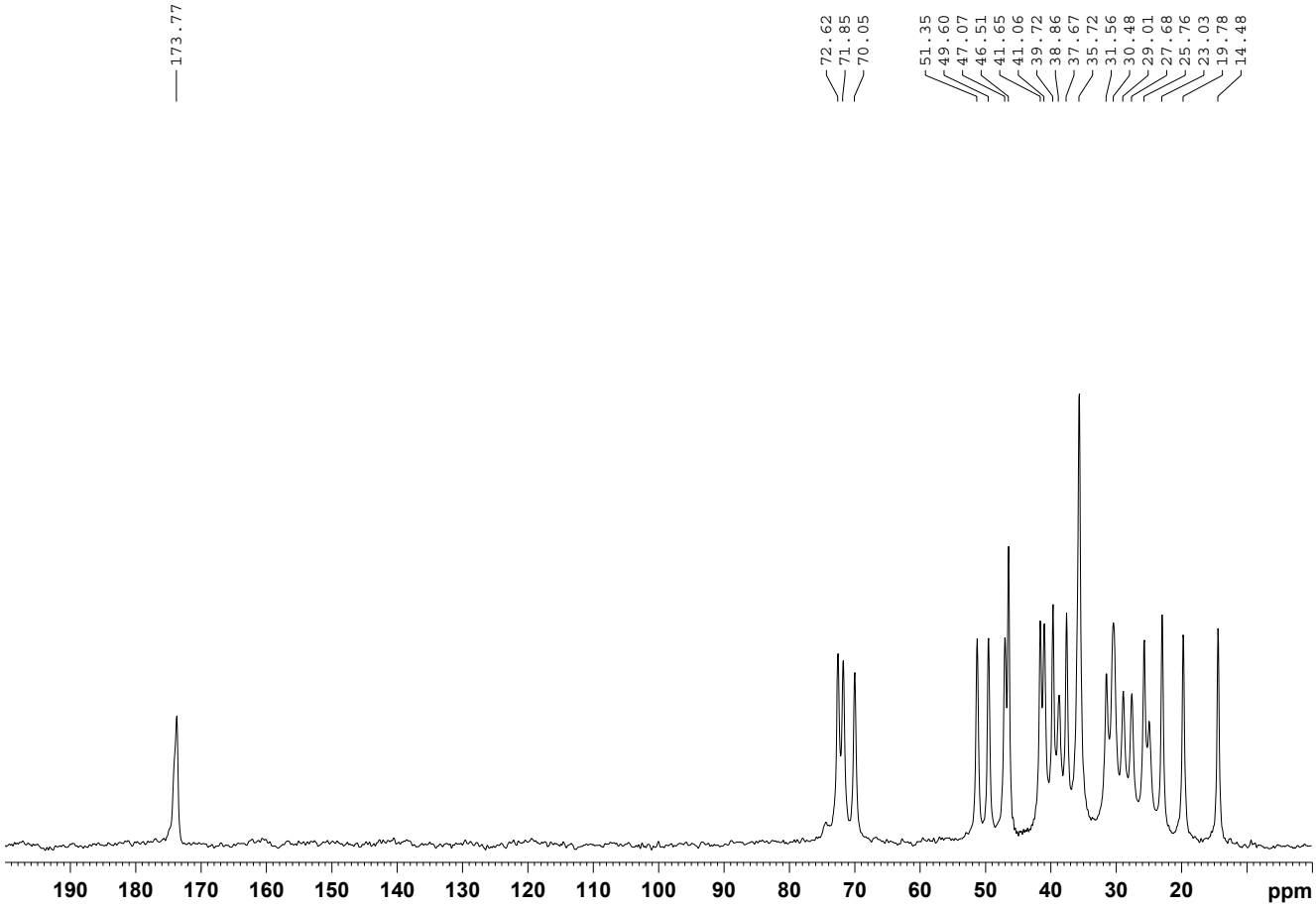

^{13}C CPMAS NMR spectra of **1** (CH_3CN Solvate)

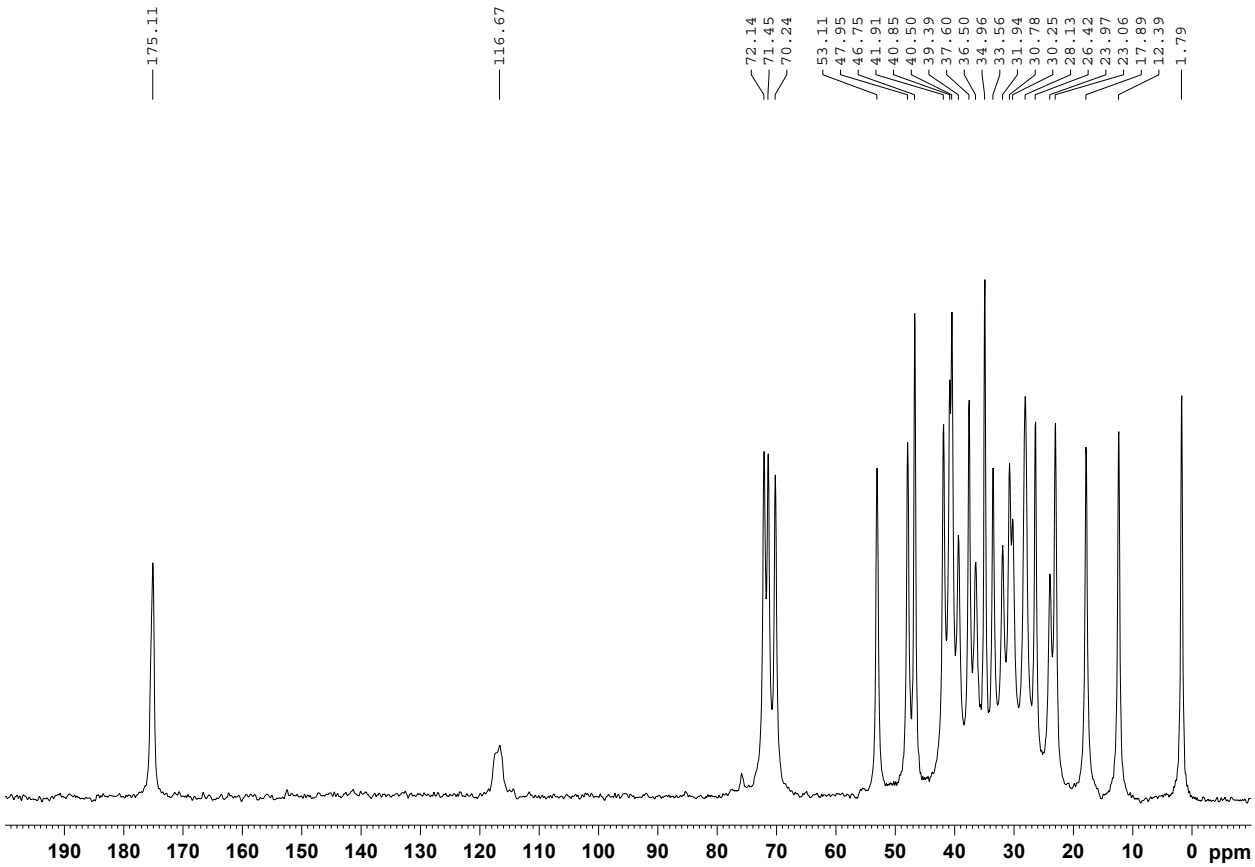

^{13}C CPMAS NMR spectra of **1** (1,2-DCB Solvate)

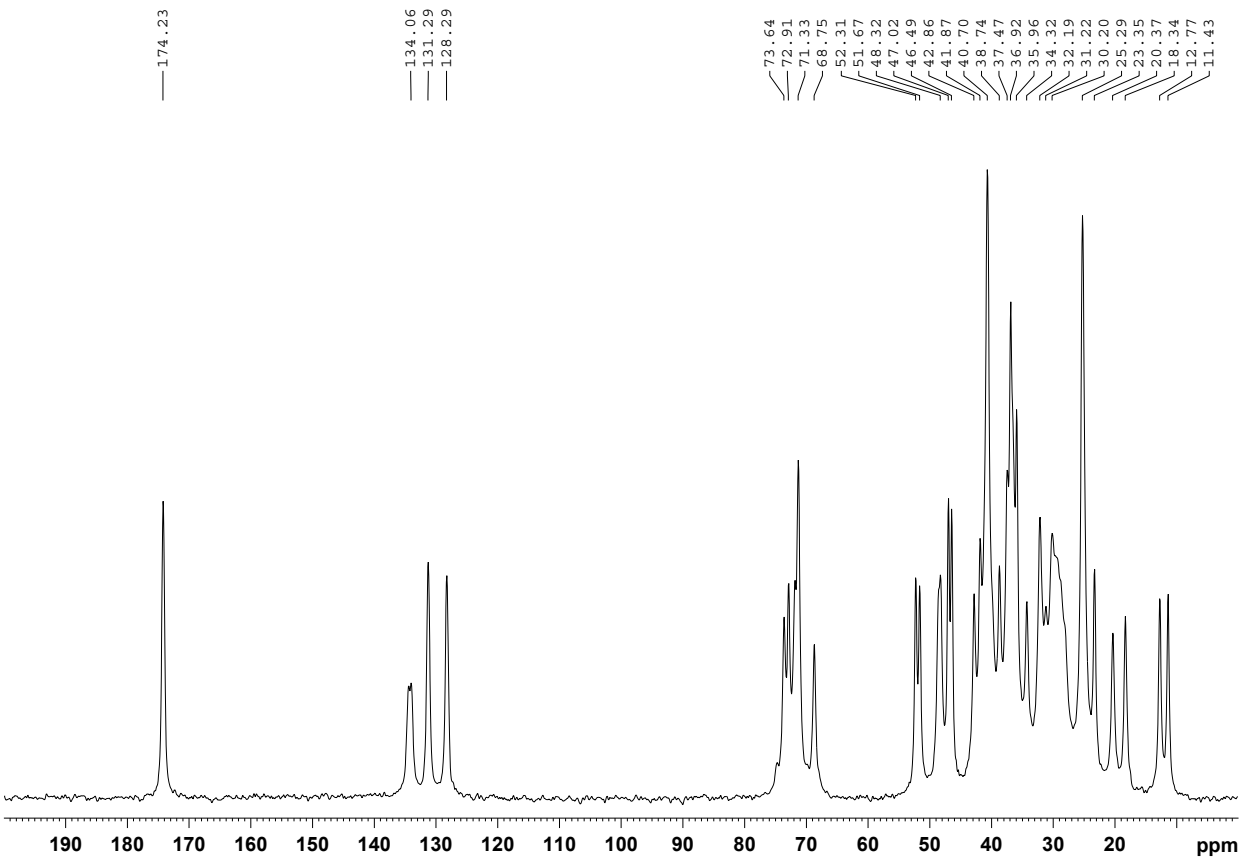

^{13}C CPMAS NMR spectra of **1** (pure form)

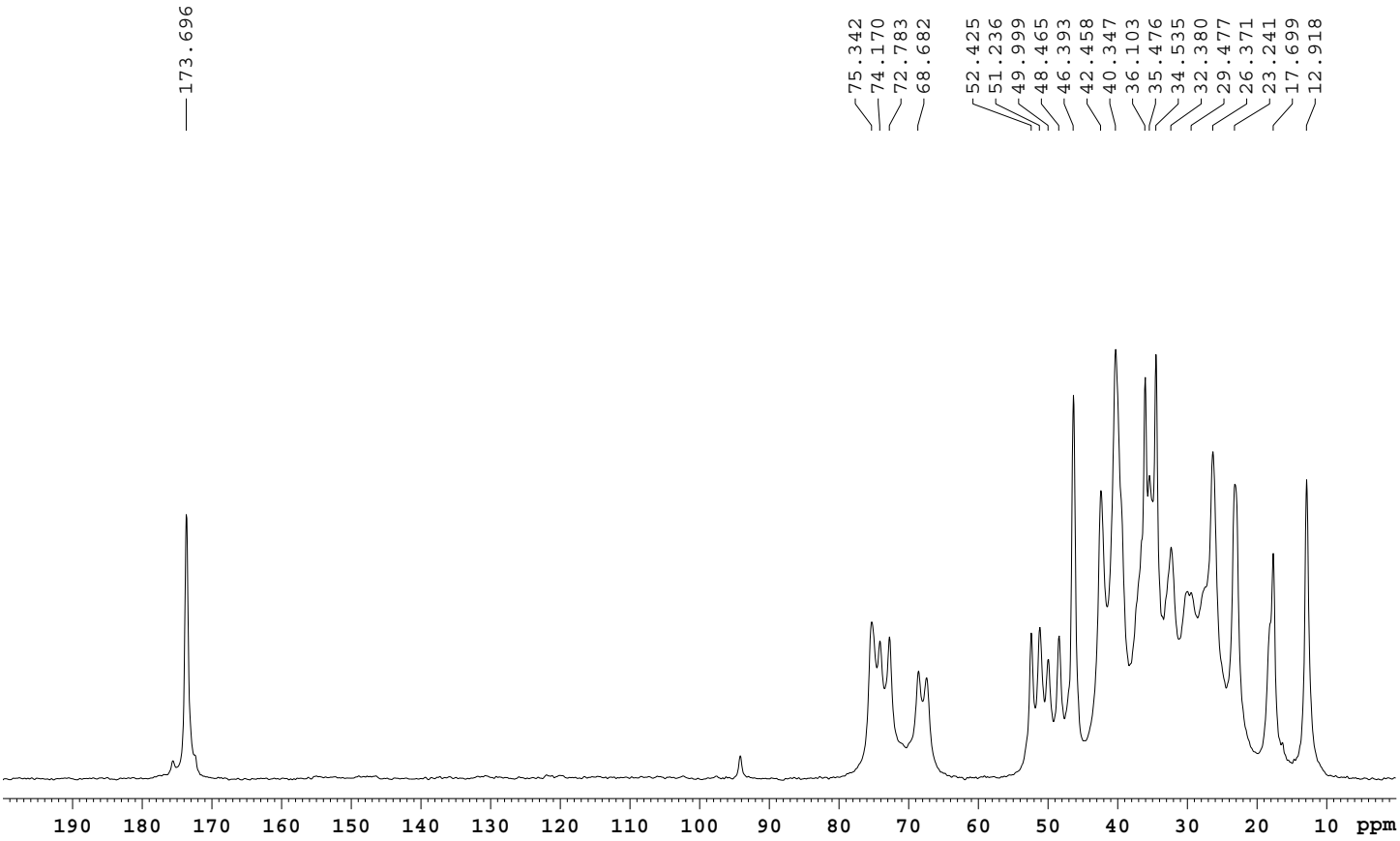

^{13}C CPMAS NMR spectra of **2**

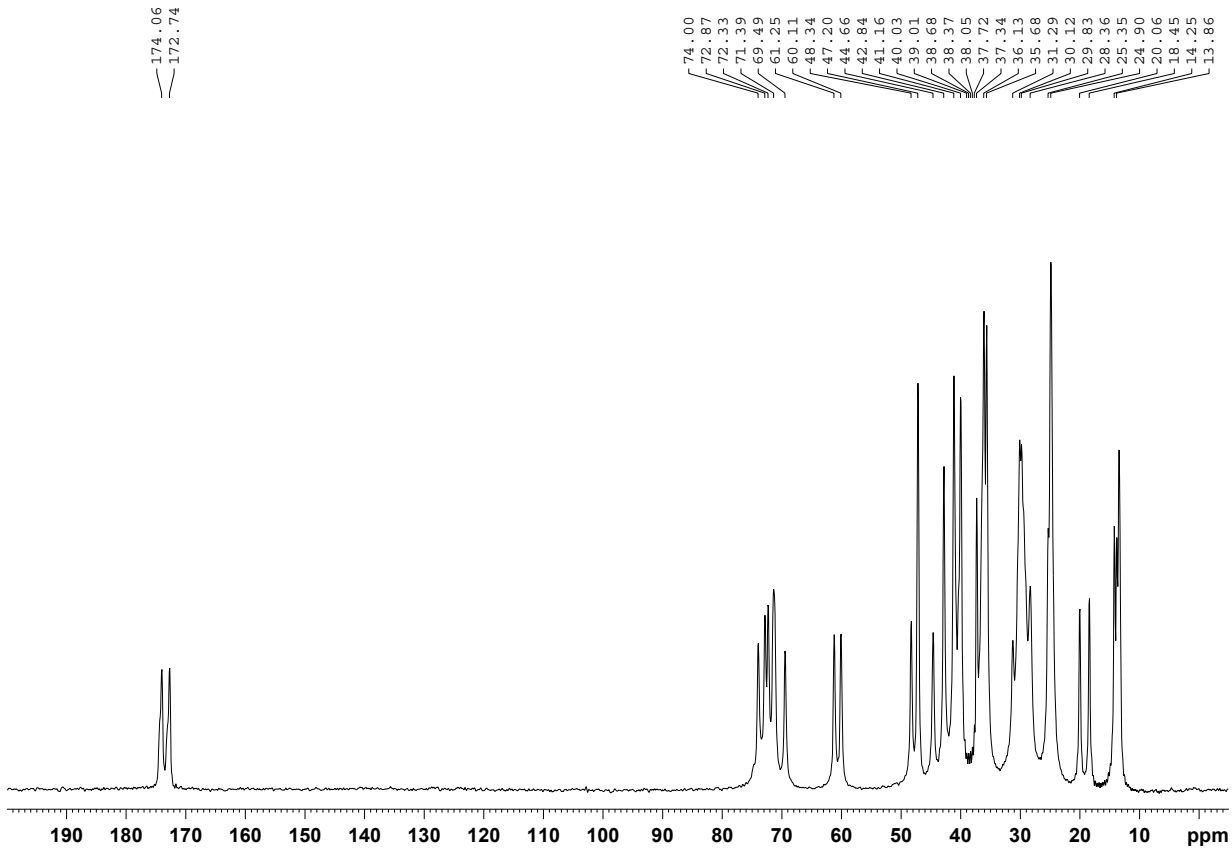

^{13}C CPMAS NMR spectra of **3**

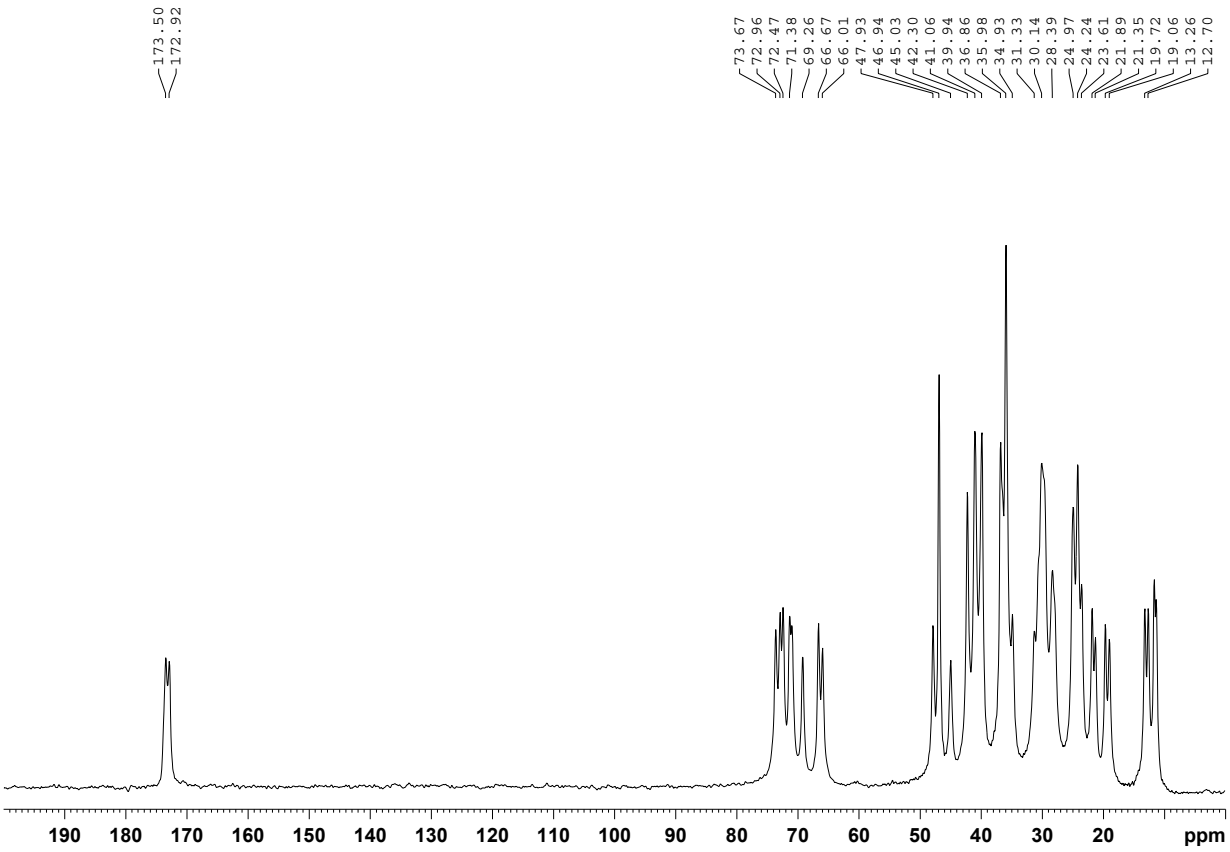

^{13}C CPMAS NMR spectra of **4**

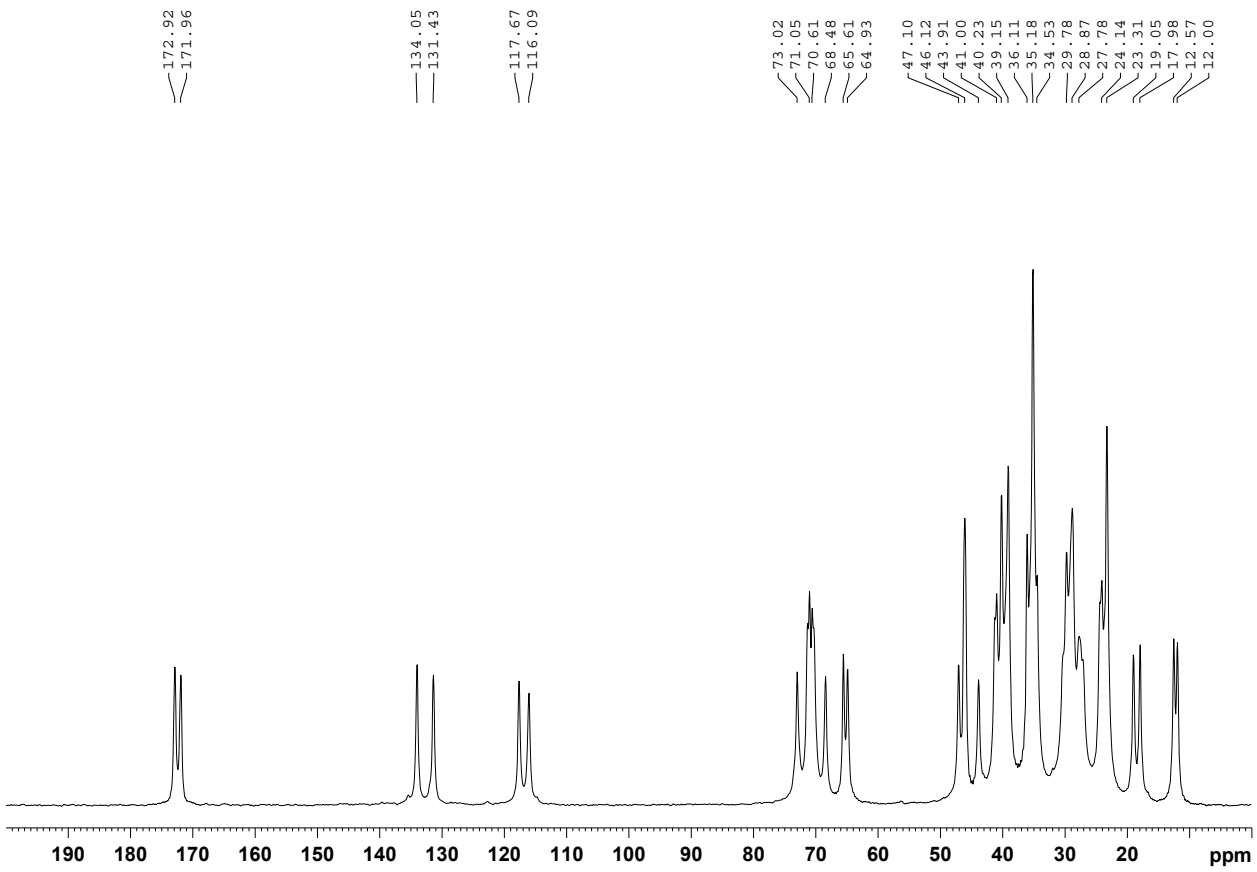

^{13}C CPMAS NMR spectra of **5**

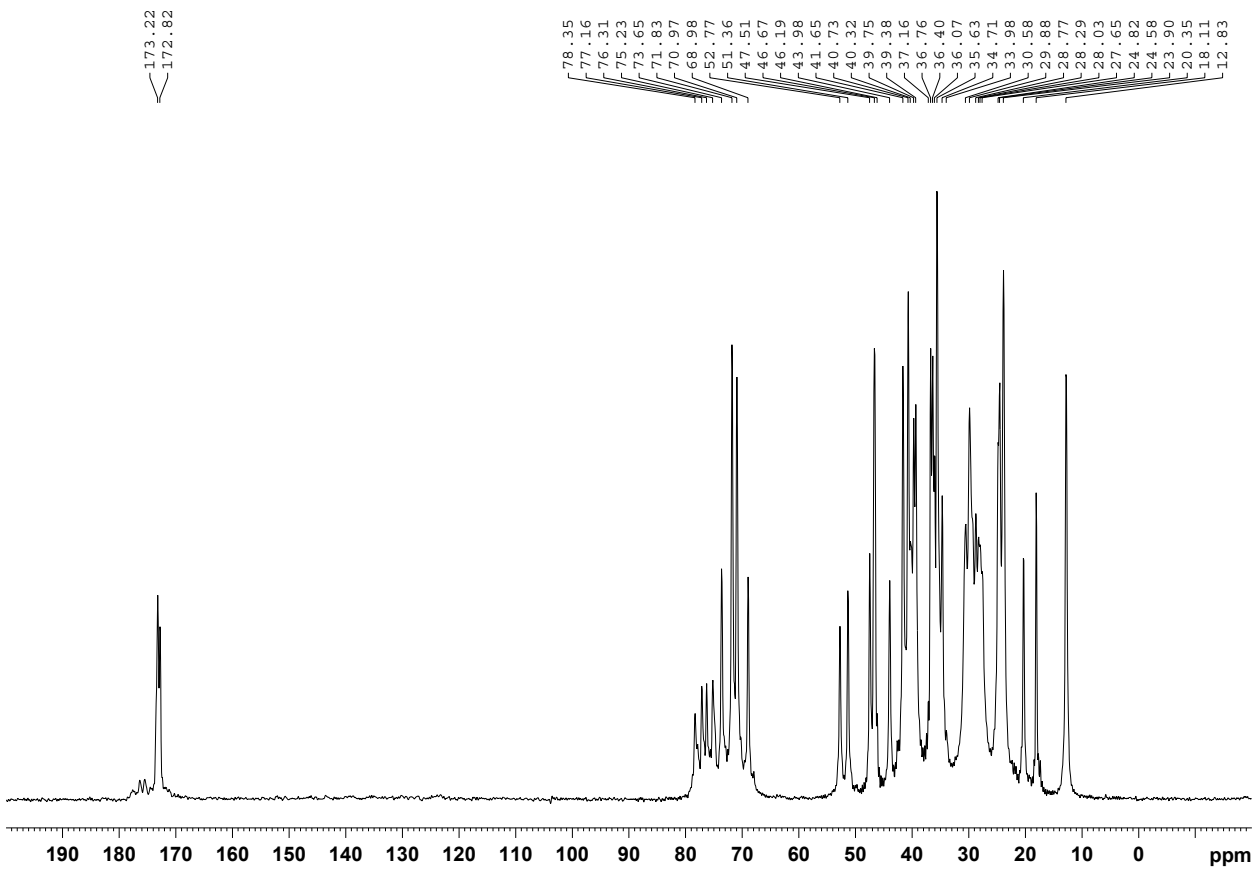

^{13}C CPMAS NMR spectra of **6**

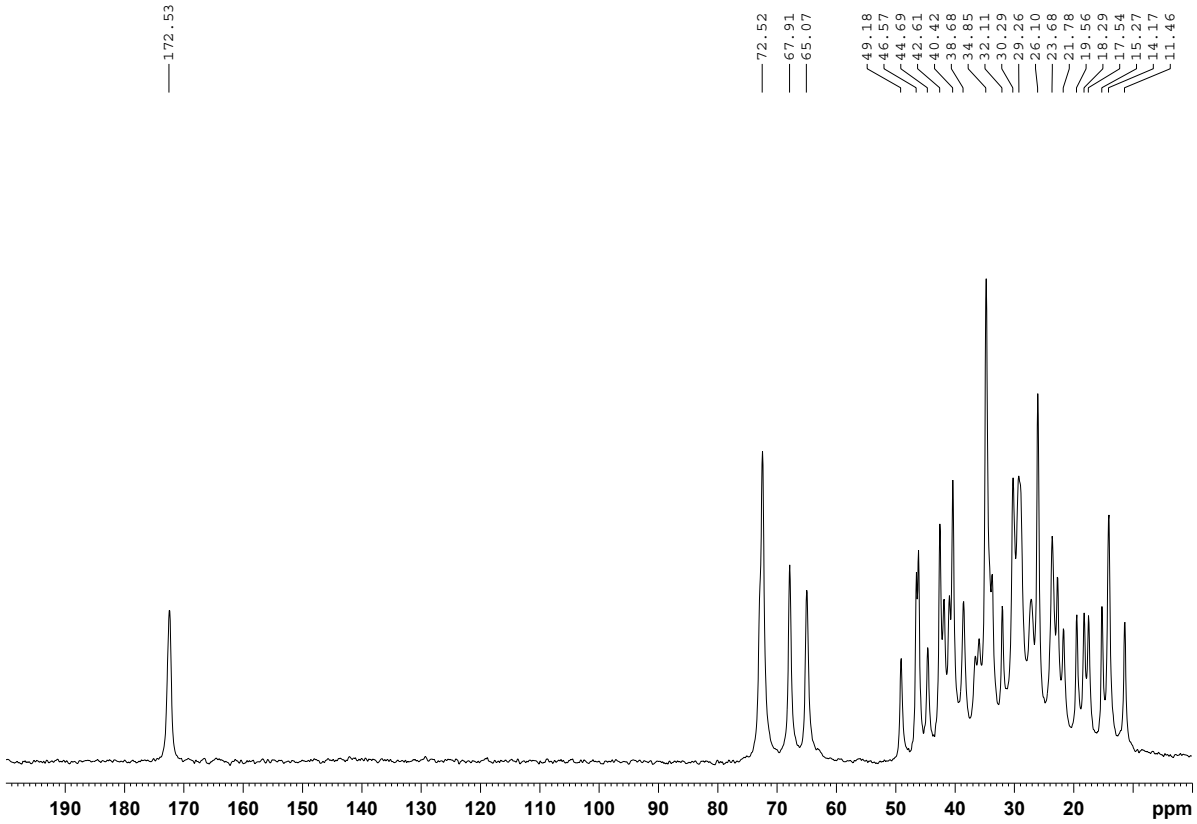

^{13}C CPMAS NMR spectra of chlorobenzene gel of **2**

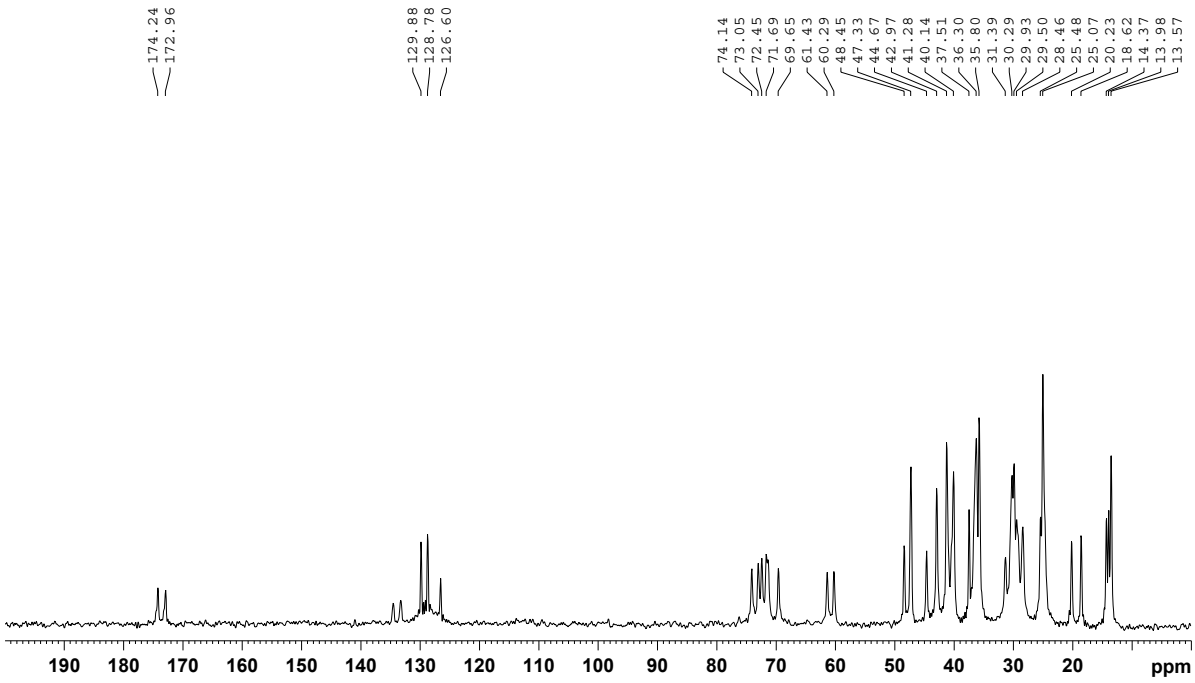

^{13}C CPMAS NMR spectra of benzene gel of **2**

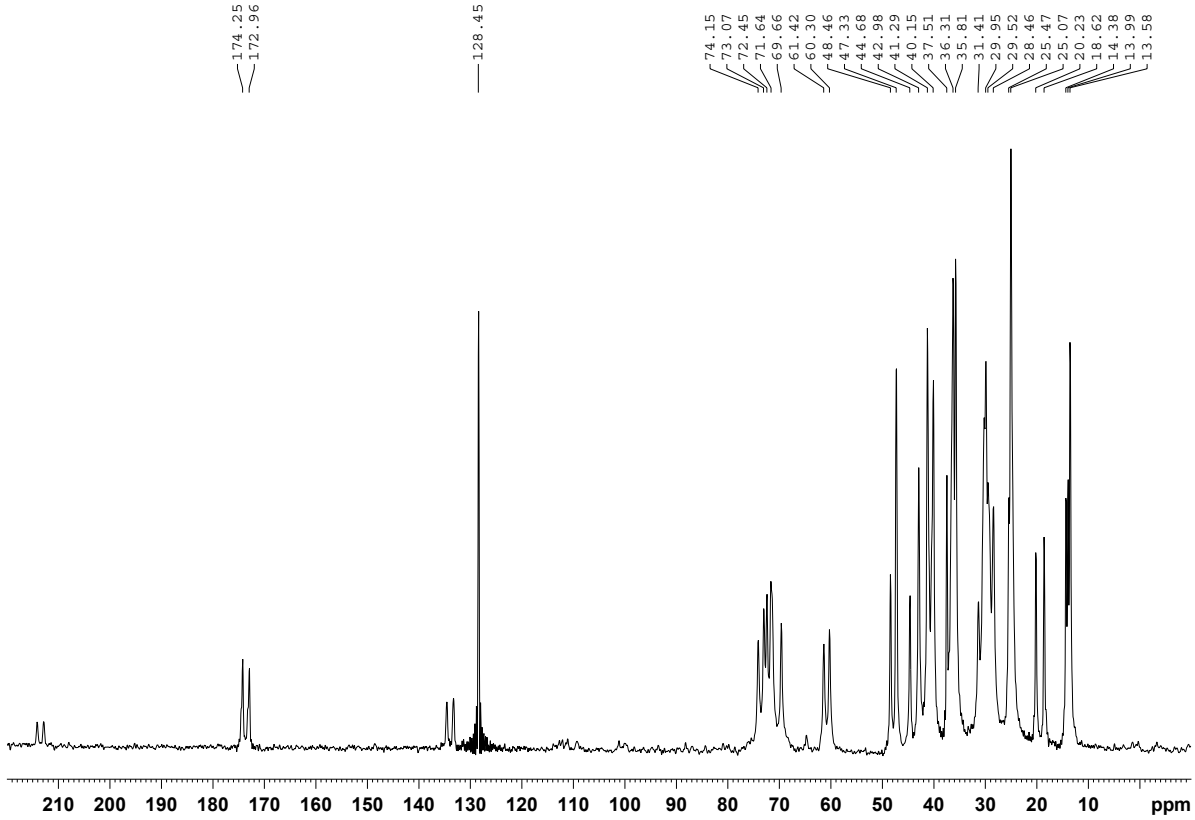

Table S4. Solution ^{13}C NMR Chemical shift values of compounds **1-6**

Carbon	**1**	**2**	**3**	**4**	**5**	**6**
1	35.24	35.23	35.32	35.26	35.26	35.32
2	30.38	30.58	30.46	30.52	30.50	30.47
3	71.82	71.97	71.91	71.93	71.91	71.92
4	39.48	39.78	39.59	39.58	39.63	39.62
5	41.60	41.49	41.70	41.80	41.77	41.73
6	34.70	34.68	34.77	34.73	34.74	34.76
7	68.34	68.36	68.45	68.42	68.42	68.45
8	39.48	39.65	39.56	39.58	39.57	39.57
9	26.20	26.73	26.43	26.52	26.49	26.45
10	34.70	34.58	34.70	34.66	34.68	34.69
11	28.15	28.37	28.21	28.28	28.27	28.22
12	72.96	72.92	73.06	73.00	73.00	73.06
13	46.38	46.54	46.47	46.49	46.49	46.47
14	41.47	41.49	41.53	41.50	41.49	41.53
15	23.14	23.17	23.22	23.19	23.19	23.22
16	27.42	27.41	27.48	27.44	27.45	27.48
17	46.94	47.21	47.09	47.10	47.06	47.10
18	12.39	12.54	12.47	12.49	12.48	12.47
19	22.40	22.55	22.47	22.48	22.48	22.47
20	35.21	35.12	35.25	35.18	35.15	35.23
21	17.23	17.35	17.32	17.33	17.30	17.32
22	31.04	31.34	31.37	31.24	31.00	31.38
23	30.87	30.91	30.98	30.89	30.75	30.97
24	174.70	174.21	174.43	173.88	173.35	174.42
25	51.35	60.17	65.85	64.92	51.73	64.12
26		14.25	22.01	132.36	77.84	26.45
27			10.38	118.04	74.67	19.15
28						13.69
Solvent peaks	116.24 1.73 (CH_3CN)					

Table S5. Solid State ^{13}C chemical shift,* values of compounds **1-6**

Carbon	**1** [a,c]	**2** [b]	**3** [b]	**4** [b]	**5** [b]	**6** [c]
1	36.50	36.12	35.59	35.14	35.59	35.95
2	30.25	30.12 29.81	30.13 29.71	30.35 29.74	30.53	30.26
3	71.45	72.31 71.48	72.43 71.34	71.00 70.57	71.78 70.92	72.47
4	39.39	41.14	41.06 39.96	40.19	39.70 39.34	40.38
5	41.91	42.82	42.31	41.29 40.96	41.60 40.69	41.87
6	34.96	37.33	35.94	34.89	34.67	34.78
7	70.24	71.32 69.49	70.97 69.21	70.31 68.44	68.94	67.88
8	39.39	40.00	39.96	39.11	40.28	40.38
9	26.42	25.35	24.98	27.07	28.84	26.05
10	34.96	35.56	36.82	36.07	36.03	36.63
11	28.13	28.33	28.40	28.83	28.73 28.25	29.00
12	72.14	74.00 72.90	73.63 72.91	72.98 71.30	73.61	72.92
13	46.75	48.31	46.90	46.08	46.63	46.16
14	40.85	41.12	41.06	40.96	41.60	40.98
15	23.97	24.85	23.61	23.67 23.27	23.85	23.64
16	26.42	28.32	28.35 27.99	27.74 27.51	27.98 27.61	27.34
17	47.95	48.31	47.88	47.06	47.47	46.54
18	12.39	13.43	13.22 12.67	12.53 11.96	12.78	11.40
19	23.06	24.90 24.06	21.84 21.31	23.67 23.27	23.85	22.74
20	34.96		34.89	35.14	35.59	34.78
21	17.89	20.04 18.45	19.68 19.02	19.00 17.94	20.31 18.07	17.50
22	31.94	31.26	31.29 30.63	30.25	30.53	33.74
23	30.78	30.13 29.81	30.10 29.62	29.74	29.84	32.04
24	175.11	174.06, 172.74	174.44 172.85	172.88 171.91	173.18 172.78	172.53
25	53.11	61.25 60.11	66.63 65.97	65.56 64.89	52.73 51.31	65.00
26		14.23 13.46	23.61	117.63 116.05	78.31 77.11	26.05

27			11.72 11.41	134.01 131.38	76.27 75.18	19.50
28						14.10
Solvent peaks	116.67 1.79					

* The chemical shift values in solid state are assigned based on ^{13}C NMR chemical shift values in solution NMR. It is known in the literature that the ^{13}C chemical shifts might deviate slightly from those in solution NMR spectra but the ^{13}C sequence assignments are still valid in solid-state NMR spectra.[2]

[a] ^{13}C data obtained from acetonitrile solvate of **1**.

[b] Compounds displaying doublet resonance pattern (gelators).

[c] Compounds displaying singlet resonance pattern (non-gelators).

References:

1. Avogardo 0.9.7, http://avogadro.openmolecules.net/wiki/Main_Page, **200**9.

2. R. A. Fletton, R. K. Harris, A. M. Kenwright, R. W. Lancaster, K. J. Packer and N. Sheppard, *Spectrochim. Acta, Part A* 1987, **43**, 1111; R. K. Harris, S. A. Joyce, C. J. Pickard, S. Cadars and L. Emsley, *Phys.Chem. Chem. Phys.* 2006, **8**, 137.